Testing the count distribution of gamma-ray sources in the extragalactic sky

Based on:

S.Manconi, M. Korsmeier, F. D., N. Fornengo, M. Regis, H.S. Zechlin

arxiv:1912.01622

Fiorenza Donato

Department of Physics, Torino University & INFN, Italy

TeVPA, Sydney - Dec 5, 2019

Emission of gamma-rays is predicted from:

- The Galactic gas (HI, HII, DNG): π^0 decay
- A Galactic Inverse Compton (IC) photon population
- An isotropic (mostly extragalactic) background
- Point sources
- Extended sources (included Fermi Bubbles and Loop I)
- Sun and Moon
- Residual Earth Limb (negligible for E> 200 MeV)

Photon statistics

pushing the γ-ray source count distribution below the Catalog detection thresholds

Zechlin, Cuoco, FD, Fornengo, Vittino ApJS 2016;
Zechlin, Cuoco, FD, Fornengo, Regis ApJ 2016, Zechlin, Manconi, FD PRD 2018

The 1-point probability distribution function (1p-PDF) :

- MEASURE the source count (N) distribution dN/dS as a function of the flux S
- EXTEND the sensitivity for dN/dS BELOW the catalog threshold
- DECOMPOSE the total gamma-ray sky into:
  - i) Point sources,
  - ii) Galactic foreground,
  - iii) Isotropic diffuse background
  - iv) Further components (i.e. dark matter)?

Dodelson, Belikov, Hooper, Serpico 2009; Malyshev&Hogg 2011; Lee, Lisanti, Safdi 2015;
Lee, Lisanti, Safdi, Slatyer 2015; Linden, Rodd, Safdi, Slatyer 2016; Vernstrom+ 2014; Vernstrom+ 2015;
Lisanti+ 2016; Leane, Slatyer 2019; Chang, Mishra-Sharma, Lisanti + 2019

1p-PDF analysis

Zechlin, Cuoco, FD, Fornengo, Vittino ApJS 2016,

1p-PDF == p_k, the probability to find k photons in a given pixel

n_k is the number of pixels counting k photons

Exploit the method of generating functions (Malyshev & Hogg 2011)

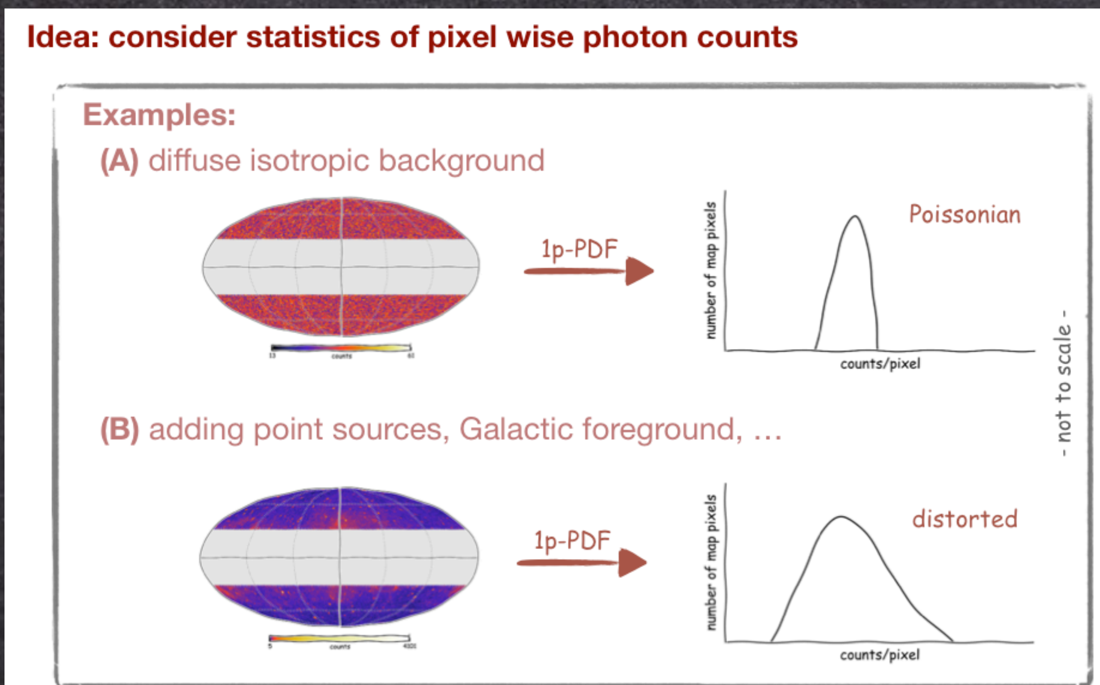

Generically, dN/dS is shaped by a multi-broken power-law (MBPL):

$$\frac{\mathrm{d}N}{\mathrm{d}S} \propto \begin{cases} \left(\frac{S}{S_0}\right)^{-n_1} & S > S_{\mathrm{b}1} \\ \left(\frac{S_{\mathrm{b}1}}{S_0}\right)^{-n_1+n_2} \left(\frac{S}{S_0}\right)^{-n_2} & S_{\mathrm{b}2} < S \leq S_{\mathrm{b}1} \\ \vdots & \\ \left(\frac{S_{\mathrm{b}1}}{S_0}\right)^{-n_1+n_2} \left(\frac{S_{\mathrm{b}2}}{S_0}\right)^{-n_2+n_3} \cdots \left(\frac{S}{S_0}\right)^{-n_{N_\mathrm{b}+1}} & \\ & S \leq S_{\mathrm{b}N_\mathrm{b}}, \end{cases}$$

Tests of the 1pPDF model

In 1-10 GeV (Zechlin+ ApJS 2016)

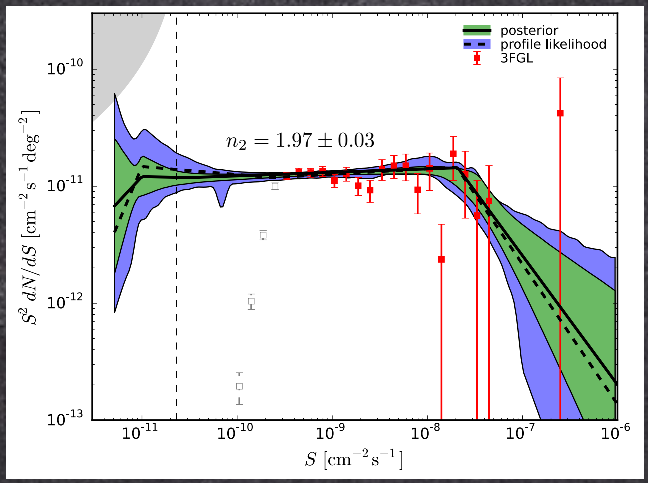

In energy bins in 1-171 GeV (Zechlin+ ApJS 2016)

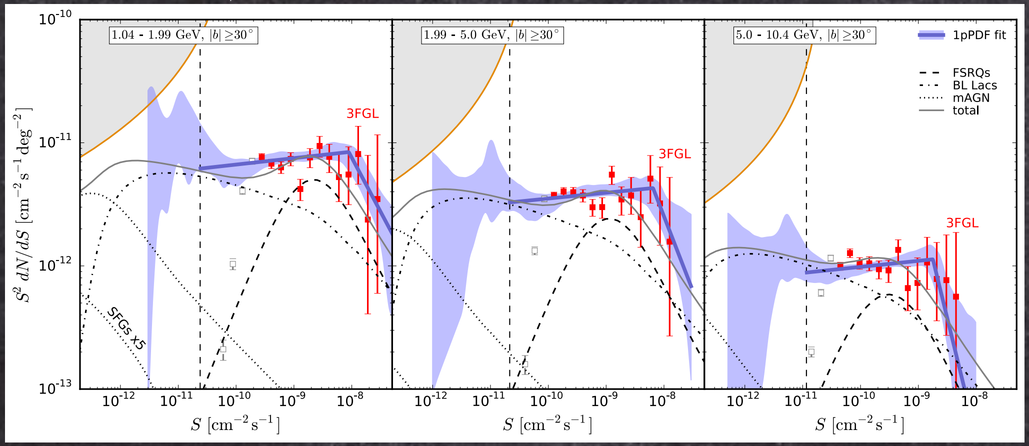

Adding a galactic dark matter template (Zechlin+ 2018)

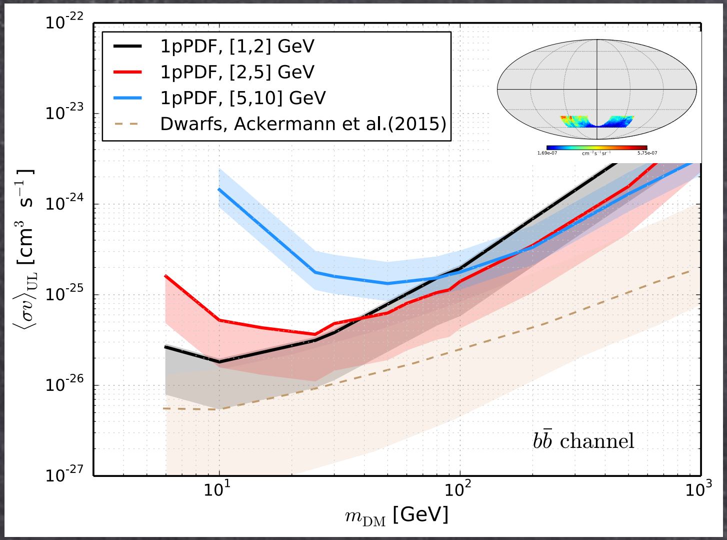

The blazar luminosity function

BLLacs & FSRQs - A unique model (Ajello + ApJL 2015)

Gamma-ray luminosity function:

$$\Phi(L_\gamma, z, \Gamma) = \Phi(L_\gamma, 0, \Gamma) \times e(L_\gamma, z)$$

$$\Phi(L_\gamma, 0, \Gamma) = \frac{A}{\ln(10) L_\gamma}\left[\left(\frac{L_\gamma}{L_0}\right)^{\gamma_1} + \left(\frac{L_\gamma}{L_0}\right)^{\gamma_2}\right]^{-1} \times \exp\left[-\frac{(\Gamma - \mu(L_\gamma))^2}{2\sigma^2}\right],$$

$$e(L_\gamma, z) = \left[\left(\frac{1+z}{1+z_c(L_\gamma)}\right)^{-p_1(L_\gamma)} + \left(\frac{1+z}{1+z_c(L_\gamma)}\right)^{-p_2(L_\gamma)}\right]^{-1}$$

$$\mu(L_\gamma) = \mu^* + \beta\left[\log\left(\frac{L_\gamma}{\mathrm{erg\ s^{-1}}}\right) - 46\right]$$

$$z_c(L_\gamma) = z_c^* \cdot (L_\gamma/10^{48})^\alpha,$$
$$p_1(L_\gamma) = p_1^* + \tau(\log(L_\gamma) - 46),$$
$$p_2(L_\gamma) = p_2^* + \delta(\log(L_\gamma) - 46).$$

The 1pPDF method with the Blazar model

$$\frac{dN}{dS} = \int_{0.01}^{5.0} dz \int_{1}^{3.5} d\Gamma\, \Phi[L_\gamma(S_{\rm E}, z, \Gamma), z, \Gamma]\, \frac{dV}{dz}\, \frac{dL_\gamma}{dS}$$

1-10 GeV
b>30 deg
10 yrs data

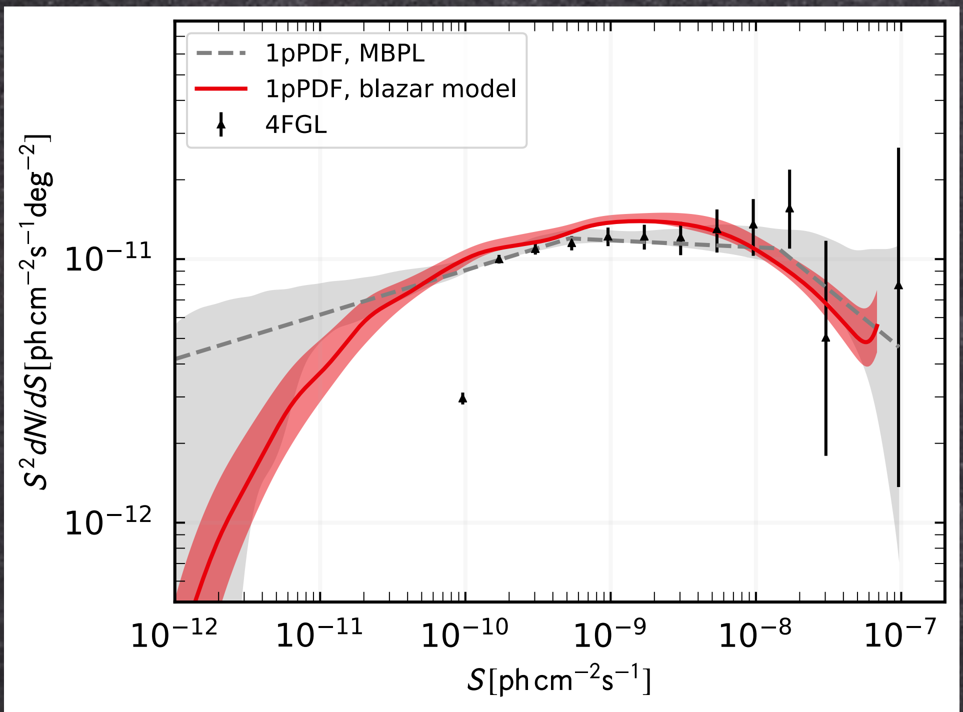

- The 1pPDF measures point sources x10 below flux threshold
- The BLAZAR model is a good fit down x100
- The BLAZAR model is compatible with 1pPDF MBPL

BTW, we also find a new fit for the MBPL dN/dS on 10 yrs and P8.

The angular power spectrum (APS) in the unresolved regime on the blazar model

$$C_{\mathrm{P}}^{i,j} = \int_{0.01}^{5.0} dz \, \frac{dV}{dz} \int_{1}^{3.5} d\Gamma \int_{L_{\min}}^{L_{\max}} dL_\gamma \, \Phi(L_\gamma, z, \Gamma) \times S_i(L_\gamma, z, \Gamma) \, S_j(L_\gamma, z, \Gamma) \, [1 - \Omega(S_{\mathrm{thr}}(L_\gamma, z, \Gamma), \Gamma)] \, . \quad (15)$$

i, j are for energy bins -> auto- and cross-correlation

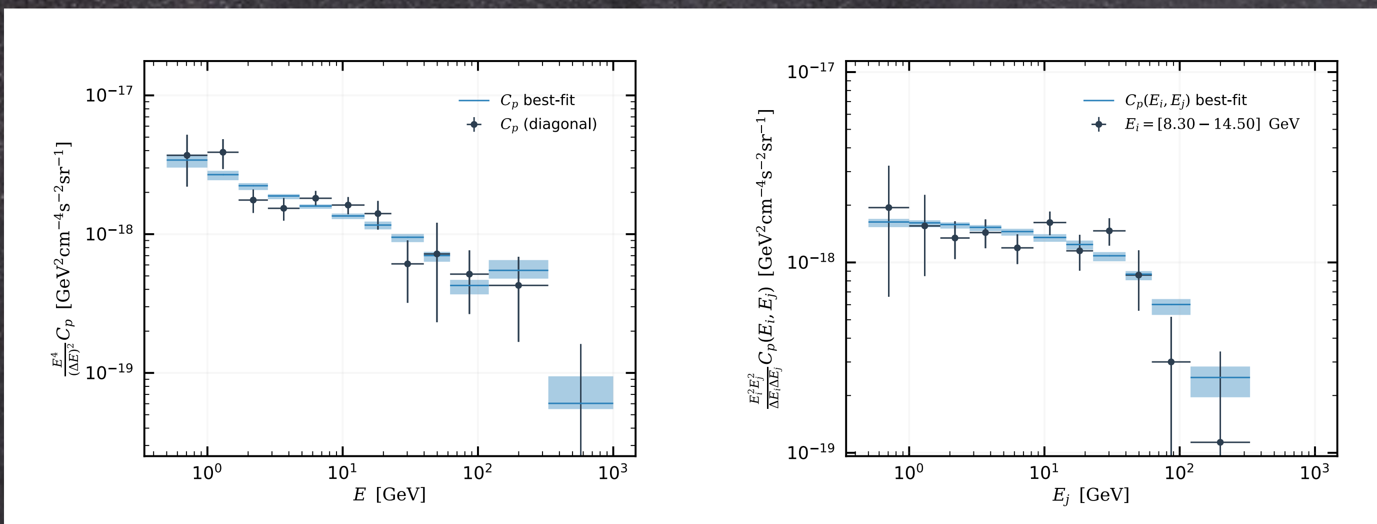

Data from Fermi-LAT PRL 2018

We find a best fit compatible with Fermi-LAT measurements and small uncertainties

The 4FGL Fermi catalog on the blazar model

This a cross check mostly (see next slide)

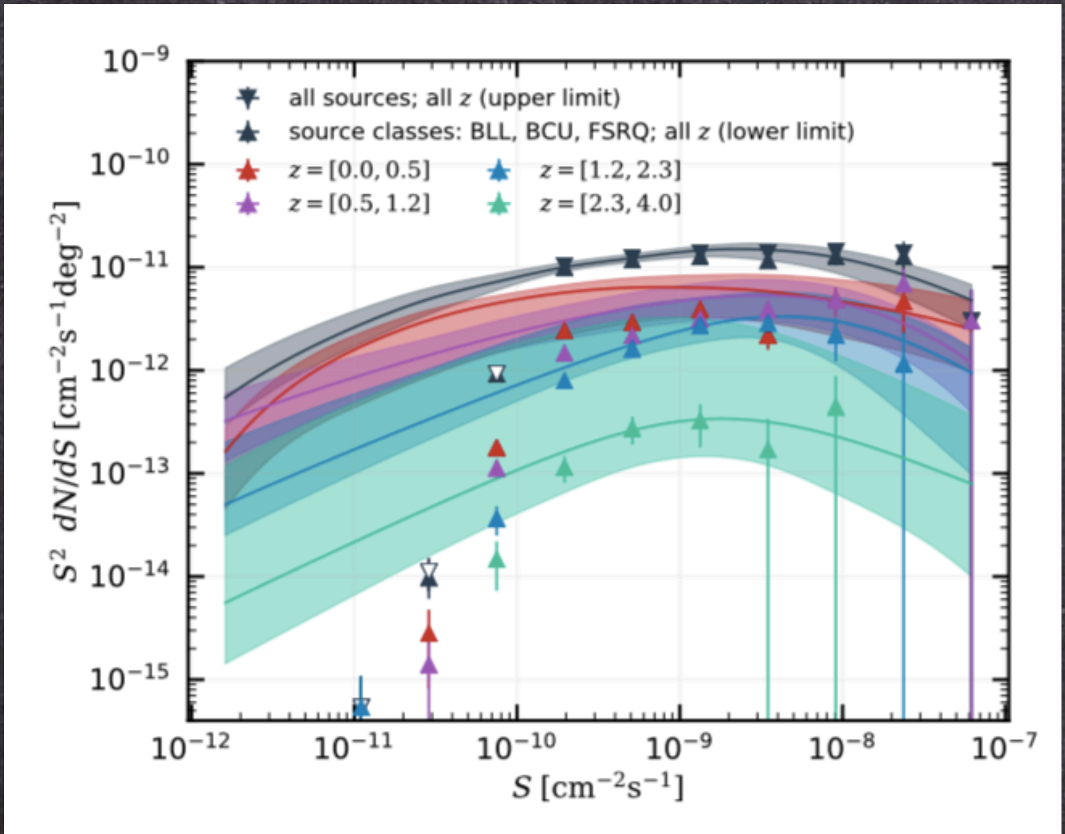

Fit of the blazar model (the 5 free parameters)

Points as lower limits due to incompleteness of catalog

Constraints to the Blazar model

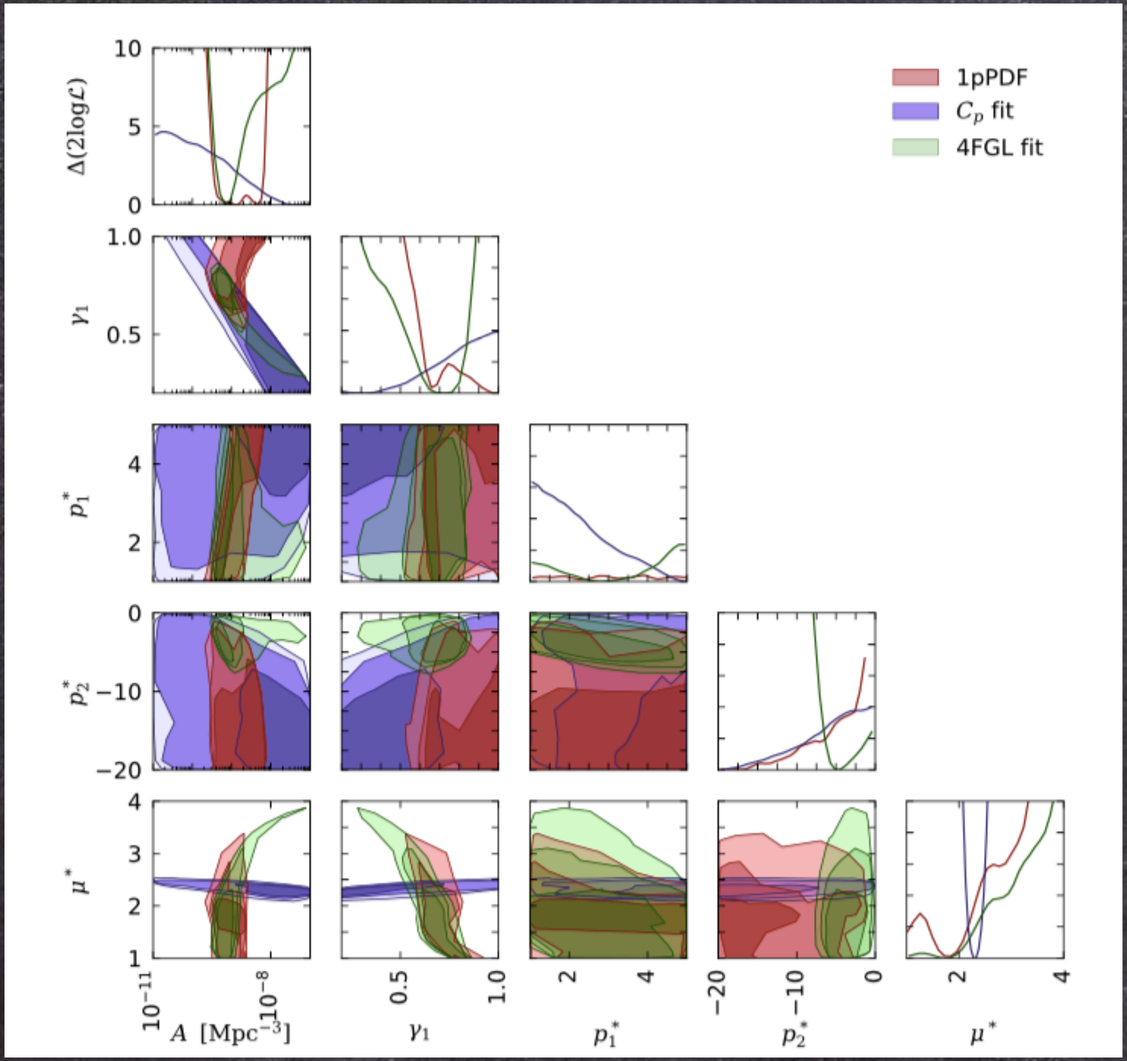

- Good compatibility 1pPDF (resolved & unresolved) and 4FGL (resolved)
- APS constrains μ^*, working on energy bins
- 1pPDF constrains A (global normalization) and γ_1 (luminosity evolution)
- Catalog bounds p_2^*

The dN/dS from the fit to 1pPDF, APS, 4FGL

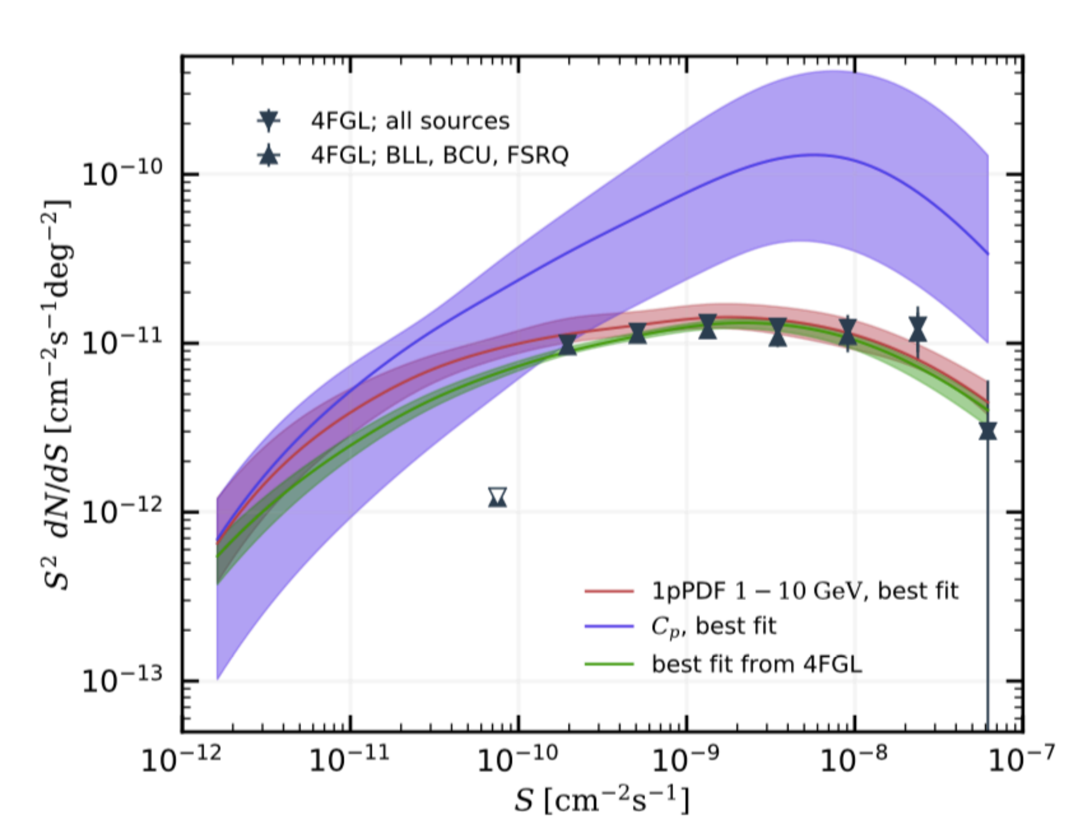

- Best fit to the resolved sources (obviously) from the catalog 4FGL
- 1pPDF constrains resolved & unresolved
- APS tests only unresolved fluxes, would over-predict resolved

The APS from the fit to 1pPDF, APS, 4FGL

The APS is an energy dependent analysis

The 1pPDF is for 1-10 GeV

The 4FGL is studied fluxes integrated 1-100 GeV

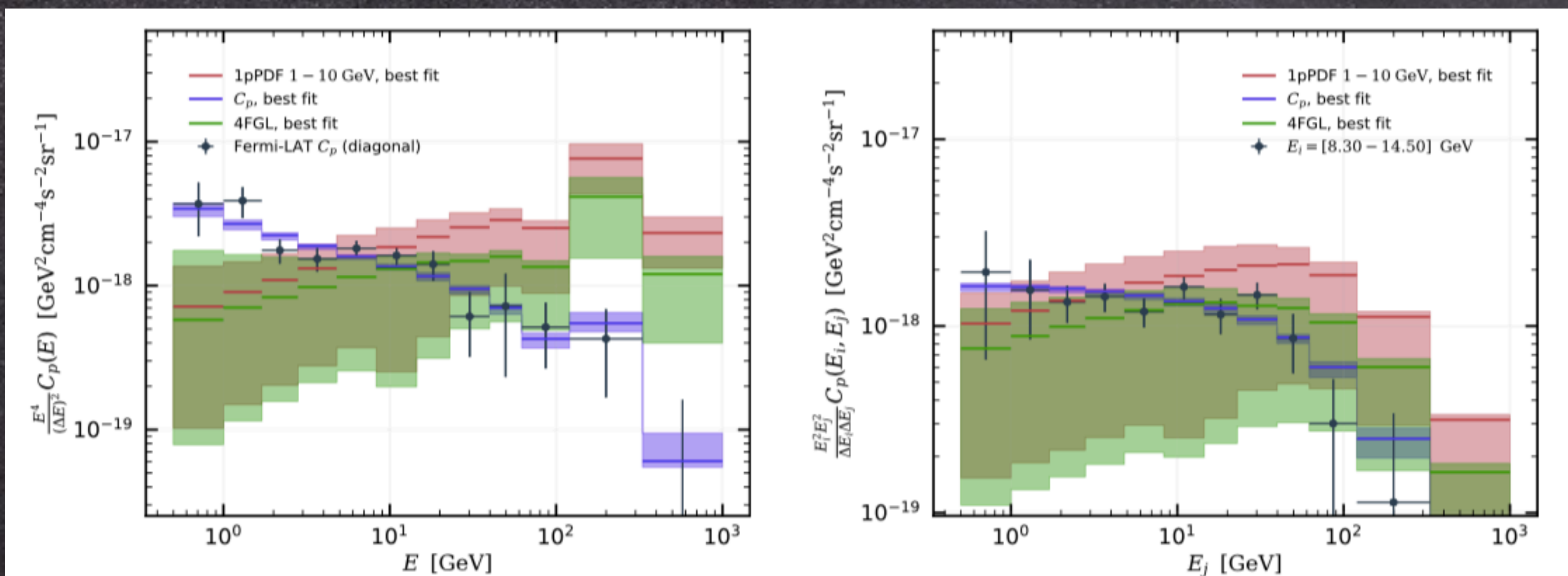

As expected, 4FGL cannot predict APS

APS and the 4FGL are complementary

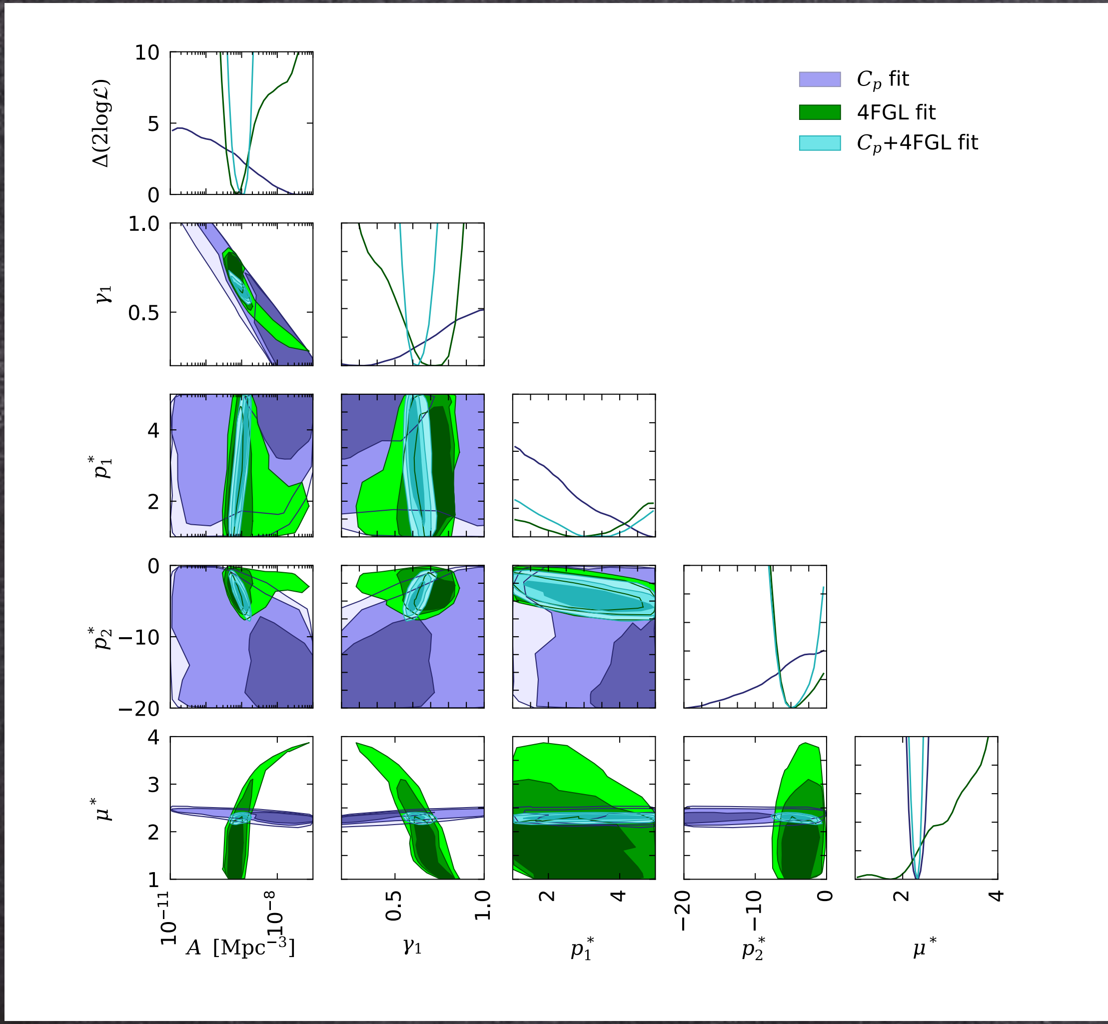

The two analysis combine to give a fit to the blazar model in both the resolved and unresolved regions

The results on the GLF

TABLE I: Best-fit parameters for each of the techniques investigated in this paper. The first column lists the free parameters, while the following four columns contain the corresponding best fits. The last column reports the reference values from Ref. [24].

Parameter	1pPDF	C_P	4FGL	C_P+4FGL	Ref. [24]
$\log_{10}(A/\mathrm{Mpc}^{-3})$	$-8.98^{+0.86}_{-0.49}$	$-7.55^{+0.54}_{-5.60}$	$-9.01^{+0.08}_{-0.19}$	$-8.91^{+0.05}_{-0.16}$	$-8.71^{+0.36}_{-0.47}$
γ_1	$0.652^{+0.44}_{-0.02}$	$0.36^{+0.17}_{-0.23}$	$0.65^{+0.16}_{-0.02}$	$0.60^{+0.04}_{-0.01}$	$0.50^{+0.14}_{-0.12}$
p_1^*	$3.26^{+2.74}_{-2.26}$	$4.89^{+0.11}_{-0.75}$	$2.80^{+1.37}_{-1.25}$	$3.74^{+0.65}_{-1.47}$	$3.39^{+0.89}_{-0.70}$
p_2^*	$-17.5^{+8.60}_{-2.54}$	$-19.5^{+7.36}_{-0.50}$	$-5.28^{+2.38}_{-0.67}$	$-5.31^{+1.57}_{-0.68}$	$-4.96^{+2.25}_{-4.76}$
μ^*	$1.78^{+0.34}_{-0.22}$	$2.32^{+0.05}_{-0.09}$	$1.79^{+0.32}_{-0.79}$	$2.31^{+0.04}_{-0.02}$	$2.22^{+0.03}_{-0.02}$
A_{gal}	$1.05^{+0.01}_{-0.01}$	-	-	-	-
F_{iso} $[10^{-7}\mathrm{cm}^{-1}\mathrm{s}^{-1}\mathrm{sr}^{-1}]$	$1.18^{+0.11}_{-0.12}$	-	-	-	-
k	-	$0.59^{+0.82}_{-0.09}$	-	$1.13^{+0.06}_{-0.05}$	-
-	$\ln(\mathcal{L})$= -245276.1	χ^2/dof =80.2/72	χ^2/dof = 5.5/2 [8]	χ^2/dof = 94.5/79	-

arxiv:1912.01622

Conclusions

- We have applied different methods to constrain the gamma-ry emission from blazars: 1pPDF (res.,unres.), APS (unres.), 4FGL (res.)

- 10 years of Fermi-LAT data at high latitude

- The 1pPDF & APS permit to fix the parameters of the gamma-ray luminosity function and SED at fluxes ~ 100 times below detector flux threshold

- The different techniques are consistent and complementary